THE OPTIMAL VECTOR PHASE MATCHING CONDITIONS IN BIAXIAL CRYSTALLINE MATERIALS DETERMINED BY THE EXTREME SURFACES METHOD: THE CASE OF MONOCLINIC CRYSTALS

DMYTRO SHULHA ¹, OLEH BURYY ², NAZARIY ANDRUSHCHAK ³, ZENOVIY KOHUT ^{1,4}, BOUCHTA SAHRAOUI ⁵, ANATOLIY ANDRUSHCHAK ^{1*}

- ¹ Department of Applied Physics and Nanomaterials Science, Lviv Polytechnic National University, Bandery Str., 12, 79013 Lviv, Ukraine
- ² Department of Semiconductor Electronics, Lviv Polytechnic National University, Bandery Str., 12, 79013 Lviv, Ukraine
- ³ Department of Computer-Aided Design Systems, Lviv Polytechnic National University, Bandery Str., 12, 79013 Lviv, Ukraine
- ⁴ Faculty of Electrical Engineering, Czestochowa University of Technology, J. Dąbrowskiego Str. 69, 42-201 Czestochowa, Poland
- ⁵ Institute of Sciences and Molecular Technologies of Angers, University of Angers, 40, rue de Rennes, BP 73532 Anger, 49035 France
- * Corresponding author: anatolii.s.andrushchak@lpnu.ua

Received: 06.11.2025

Abstract. The optimal geometries of vector phase matching are determined for the cases of second harmonic, sum, and difference frequency generation in monoclinic nonlinear optical crystals, namely $GdCa_4O(BO_3)_3$, $YCa_4O(BO_3)_3$ (point group of symmetry m), BiB_3O_6 , and $La_2CaB_{10}O_{19}$ (point group of symmetry 2). The extreme surface technique was used to determine the directions of the wave vectors that yield the highest achievable generation efficiency. The obtained results are compared with the ones for scalar phase matching. It is shown that vector phase matching increases the efficiency by tens of percent compared to the scalar case (about 53% for the BiB_3O_6 crystal). BiB_3O_6 reveals the highest absolute values of the efficiency, whereas the lowest ones are by the $La_2CaB_{10}O_{19}$ crystal.

Keywords: monoclinic crystals, second harmonic generation, sum-frequency generation, difference frequency generation, biaxial crystals, interaction geometry, extreme surfaces

UDC: 535.18

DOI: 10.3116/16091833/Ukr.J.Phys.Opt.2025.04095

This work is licensed under the Creative Commons Attribution International License (CC BY 4.0).

1. Introduction

Determining the maximum theoretically achievable values of certain effects in crystalline materials is an important problem from an applied perspective, with solutions indicating ways to increase the efficiency of material use in devices. If the value of the effect, the maximum (in certain applications, possibly the minimum) of which is sought, does not depend on the geometric characteristics of the device, the absolute values of the applied loads, etc., it can be considered as a characteristic of the material and used for comparison with other materials.

In nonlinear optics problems, the conversion efficiency can be considered a characteristic, or rather a component separated from it, depending only on the wave directions and the material parameters. In our previous papers [1,2], we studied the maximum achievable efficiencies of second-harmonic (SHG), sum-frequency (SFG), and

difference frequency (DFG) generation in uniaxial and biaxial (orthorhombic) crystals. The highest achievable value was determined by optimizing the propagation directions of the interacting waves, which were generally considered non-collinear; in other words, the vector phase matching (PM) case was analyzed. In such a more general formulation of the problem, this analysis was carried out for the first time. In this work, we extend our approach to lower-symmetry nonlinear optical crystals of the monoclinic system. The nomenclature of such crystals is not significant: as far as we know, only for four of them – $GdCa_4O(BO_3)_3$ (GdCOB), $YCa_4O(BO_3)_3$ (YCOB), $YCa_4O(BO_3)_3$ (YCOB), YCOB), YCOB, YCOB,

2. Basic relations and parameters of crystals

As it is known, the total efficiency of the nonlinear three-wave mixing processes (see, e.g., [6,7]) is proportional to the geometrical factor:

$$\eta = \frac{\left(\vec{e}_3 d\vec{e}_1 \vec{e}_2\right)^2}{n(\lambda_1) n(\lambda_2) n(\lambda_3)},\tag{1}$$

where λ_i are the wavelengths, \hat{d} is the tensor of nonlinear coefficients, $n(\lambda_1)$, $n(\lambda_2)$, $n(\lambda_3)$ are the refraction indices of pump (1, 2) and output (3) beams, \vec{e}_1 , \vec{e}_2 , \vec{e}_3 are the unit vectors parallel to the electric vectors of the corresponding waves, $\vec{e}_j = \hat{\epsilon} \vec{i}_j$, $\hat{\epsilon}$ is the dielectric permittivity tensor, \vec{i}_j is the electric displacement unit vector [8]. The dimension of η is pm²/V², and it represents only the geometrical factor of the total efficiency of nonlinear optical process. This factor is determined by crystals symmetry and the relationship between the nonlinear coefficients. It allows one to construct extreme surfaces representing the highest achievable values of η for all possible directions of the output wave vector \vec{k}_3 , determined by the angles θ , φ of the spherical coordinate system (CS). Since this paper is devoted to the characteristics of materials, the efficiency in the form (1), which does not account for the length of the nonlinear medium or the powers of the interacting waves, is convenient for our analysis.

In the case of the strict vector PM, the following expression for the wave vectors should be satisfied:

$$\vec{k}_3 = \vec{k}_1 \pm \vec{k}_2,\tag{2}$$

where the upper sign corresponds to SHG or SFG and the lower sign to DFG. As well as in [1,2], in our calculations, the wave vector \vec{k}_3 is passed through the full spherical angle $(\theta=0...\pi,\, \varphi=0...2\pi)$. For each given \vec{k}_3 , the condition (2) can be fulfilled for a set of \vec{k}_1 , \vec{k}_2 pairs, and the value of the efficiency η is generally different for different \vec{k}_1 , \vec{k}_2 . Thus, for

each \vec{k}_3 , we determine such a \vec{k}_1 , \vec{k}_2 pair that maximizes the efficiency; as a result, the dependence η_{\max} (\vec{k}_3) is obtained, which can be represented by a surface. Because each point of this surface is obtained after optimization, we call it the extreme one. The highest value of η_{\max} (designed further as $\eta_{\text{vect}}^{\text{extr}}$) is the sought value of the maximal achievable efficiency, the determination of which is the objective of our work. A more detailed explanation of the optimization technique for the case of biaxial crystals is given in [2]. The analysis of the scalar PM was also carried out for comparison, and the corresponding maximal achievable efficiency for scalar case $\eta_{\text{scal}}^{\text{extr}}$ was determined.

All calculations for SHG and SFG were carried out for two types of PM determined by the velocities (and polarizations) of interacting beams: (i) both pump waves are 'slow', i.e. correspond to higher value of the refraction index (of two possible for a given direction of the wave vector), and the output wave is 'fast' (ssf or type I PM) and (ii) one pump wave is slow and the other is fast (sff. fsf or type II PM). For DFG in biaxial crystal type I, PM is ffs, and for type II, it is fss or fsf. The mutual orientations of the wave vectors of the pump \vec{k}_1 , \vec{k}_2 , and output \vec{k}_3 waves for the case of SFG are shown in Fig. 1.

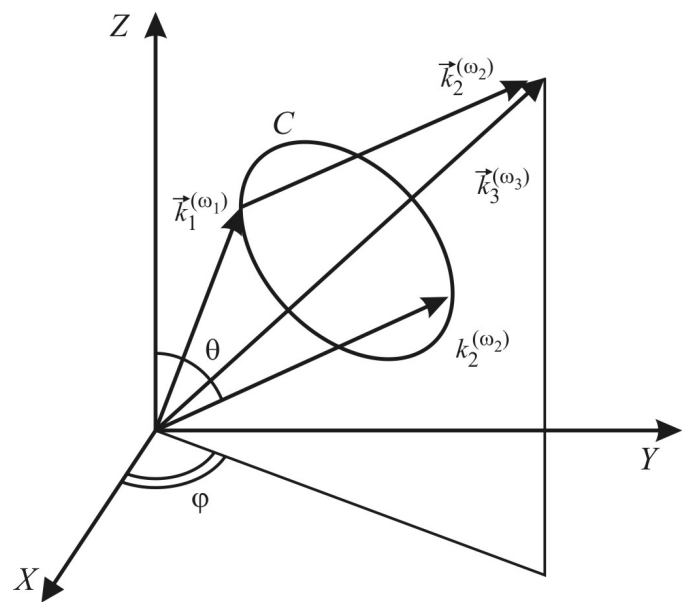


Fig. 1. The mutual orientations of the wave vectors of the pump \vec{k}_1 , \vec{k}_2 and output \vec{k}_3 waves (the case of SFG); C is the line of cross-section of wave vector surfaces of initial waves (see [2] for details).

The extreme surfaces are constructed, and optimal PM conditions are determined for GdCOB, YCOB, BiBO, and LCB crystals that belong to the point symmetry groups of symmetry m or 2 (the third point group of the monoclinic symmetry (2/m) is centrosymmetric, so the considered effects are not observed in crystals of this group). The nonlinear susceptibilities of the crystals taken from [3-5] are indicated in Table 1. It should be noted that nonlinear susceptibilities were not measured for the LCB crystal, and only the calculated values are known for it [5]. However, as shown in Table 1, these values of the nonlinear susceptibilities do not satisfy the Kleinman symmetry rule ($d_{14} = d_{25} = d_{36}$, $d_{16} = d_{21}$, $d_{23} = d_{34}$). Nevertheless, the Kleinman symmetry can be violated (e.g., Ukr. J. Phys. Opt. 2025, Volume 26, Issue 4

for BiBO); in the case of LCB, this violation is significant – the corresponding coefficients differ even in sign. Even though this casts doubt on the accuracy of the coefficient determination in [5], we have also performed calculations for such values, since for monoclinic crystals of point group 2, the amount of appropriate data is limited.

The refractive indices were calculated using the Sellmeier equations given in [3]. All extreme surfaces were constructed in a crystal-optics CS connected with the output light wave, i.e., the orthogonal system was built on the main axes of the optical indicatrix (where the X axis corresponds to the lowest value of the main refraction index, the Y axis to the intermediate, and the Z-axis to the highest one). Because the components of the tensor of nonlinear coefficients d for the BiBO crystal are given in a special orthonormalized crystal-physics CS that differs from the crystal-optics one (see Fig. 2), the tensor transformations were carried out in accordance with known rules [9,10]. For GdCOB and YCOB crystals, the crystal-physics CS coincides with the crystal-optics one [11,12]. The orientation of the axes for LCB is not described; however, it is known that the crystal-optic system for the crystal is similar to the ones of GdCOB and YCOB, particularly, the Y axis coincides with the crystallographic axis b [13-15].

Table 1. Parameters of the considered crystals.

Crystal	Nonlinear susceptibilities, d_{ij} , pm/V	
	Point group of symmetry m	
GdCOB*	$d_{11} \approx 0$; $d_{12} = d_{26} = 0.27$; $d_{13} = d_{35} = -0.85$; $d_{31} = d_{15} = 0.20$;	
	$d_{32} = d_{24} = 2.23; d_{33} = -1.87$	
YCOB*	$d_{11} \approx 0$; $d_{12} = d_{26} = 0.24$; $d_{13} = d_{35} = -0.73$; $d_{31} = d_{15} = 0.41$;	
	$d_{32} = d_{24} = 2.35$; $d_{33} = -1.60$	
	Point group of symmetry 2	
BiBO	$d_{14} = 2.4$; $d_{16} = 2.8$; $d_{21} = 2.3$; $d_{22} = 2.53$; $d_{23} = -1.3$;	
	$d_{25} = 2.3$; $d_{34} = -0.9$; $d_{36} = 2.4$	
LCB	$d_{14} = -0.05$; $d_{16} = -0.15$; $d_{21} = 0.55$; $d_{22} = -0.25$; $d_{23} = 0.4$;	
	$d_{25} = 0.02$; $d_{34} = -0.25$; $d_{36} = -0.05$	

^{*}Given equalities of the nonlinear susceptibilities for GdCOB and YCOB correspond to the Kleinman symmetry conditions, which are valid for these crystals [4].

Moreover, the principal axes of the indicatrix do not coincide for different wavelengths, which should also be taken into account. However, sufficiently complete information for this is known only for BiBO [4,10]; for other crystals, we neglect this difference in the calculations. As shown below, such an approximation is quite acceptable for BiBO, although its validity for other crystals requires further investigation.

The wavelength dependence of the angle ϕ between abscissa axes of crystal-physics and crystal-optics CS for BiBO was determined in [8] for certain values of λ in the range of 0.365...2.325 μ m. Since our calculations require values of this angle at arbitrary wavelengths, we approximated the dependence found in [10]. As it is seen from Fig. 3, it is well described by the function:

$$\phi(\lambda) = \frac{\lambda - a}{b_0 + b_1(\lambda - a) + b_2(\lambda - a)^2},$$

$$[\lambda] = \mu m, \quad a = 0.215 \pm 0.009 \,\mu m, \quad b_0 = (3.8 \pm 0.3) \times 10^{-4} \,\mu m/deg,$$

where

 $[\varphi]$ =degrees,

 $b_1=0.02023\pm7\times10^{-5}$ deg⁻¹, $b_2=(6.5\pm0.3)\times10^{-4}$ (µm×deg)⁻¹.

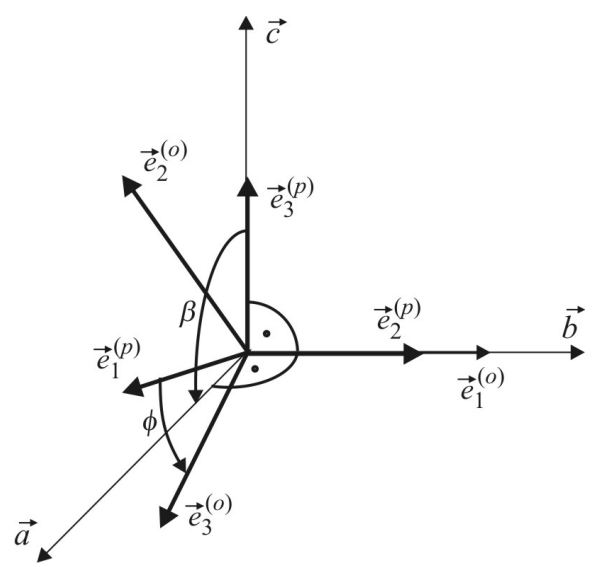


Fig. 2. The mutual orientations of the crystallographic CS (the unit vectors \vec{a} , \vec{b} \vec{c} , the angle between \vec{a} and \vec{c} is $\beta=105.62^{\circ}$ [4]), crystal-physics CS (the unit vectors $\vec{e}_i^{(p)}$, i=1,2,3), and crystal-optics CS (the unit vectors $\vec{e}_i^{(o)}$, i=1,2,3) for the BiBO crystal. The nonlinear susceptibilities were determined in the crystal-physics CS [9], however, in accordance with the algorithm used for calculations, the minimal main value of the refraction index must correspond to the abscissa axis, which is why the unit vector $\vec{e}_1^{(o)}$ of the crystal-optics CS coincides with $\vec{e}_2^{(p)}$ of the crystal-physics one. The orientations of other axes of crystal-optics CS is shown in accordance with [9].

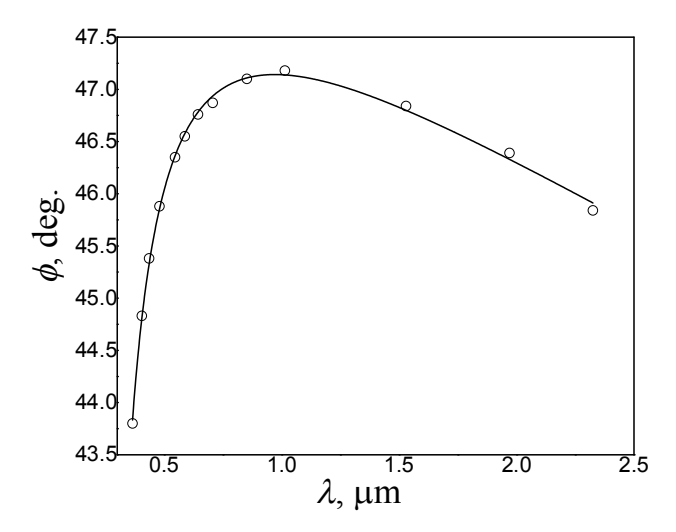


Fig. 3. The dependence of the angle ϕ (deg) on the wavelength (μ m) for the BiBO crystal (circles) [8] and its approximation by the function (3) (line).

At that, with the known values of ϕ , the components of dielectric permittivity tensors for input waves were determined in the crystal-optics CS connected with the output beam in accordance with known rules [6]. Because the directions of the

Y-axes (unit vector $\vec{e}_1^{(o)}$) of indicatrices for all wavelengths coincide for the BiBO crystal, only one non-zero non-diagonal component ϵ_{23} appeared as a result of such a tensor transformation.

3.3. Results and Discussion

3.1. Second-harmonic generation

The wavelengths of pump beams used in the calculations of the maximal achievable SHG efficiency are equal to $1.0642 \mu m$ for all considered crystals.

The general and the top views of extreme surfaces of the SHG efficiency η_{max} for the investigated crystals are shown in Figs. 4,5. The black lines on the figures correspond to the scalar PM conditions. It should be noted that the point (0;0;0), as well as the lines connecting this point with the edges of the extreme surface, do not belong to this surface and appear in the figures only in connection with the method of 3D surface construction in the software used.

Because the condition (2) is not fulfilled for type II PM in GDCOB at the considered wavelength, only one extreme surface (for ssf PM) is shown for this crystal. As it is seen from Figs. 1,2, the forms of ssf extreme surfaces are similar for GdCOB and YCOB (belonging to the point group of symmetry m) crystals. In contrast, for BiBO and LCB (belonging to the point group of symmetry 2), they are essentially different. Obviously, it is caused by different coordinate transformation rules for BiBO and LCB, and by different relationships among the values of the nonlinear susceptibilities d_{ij} .

The values shown in the parentheses in the last column of Table 2 are the relative increase of SHG efficiency caused by vector PM in relation to the scalar one, $\gamma = (\eta_{\text{vect}}^{\text{extr}} - \eta_{\text{scal}}^{\text{extr}}) / \eta_{\text{scal}}^{\text{extr}}$ (in percents).

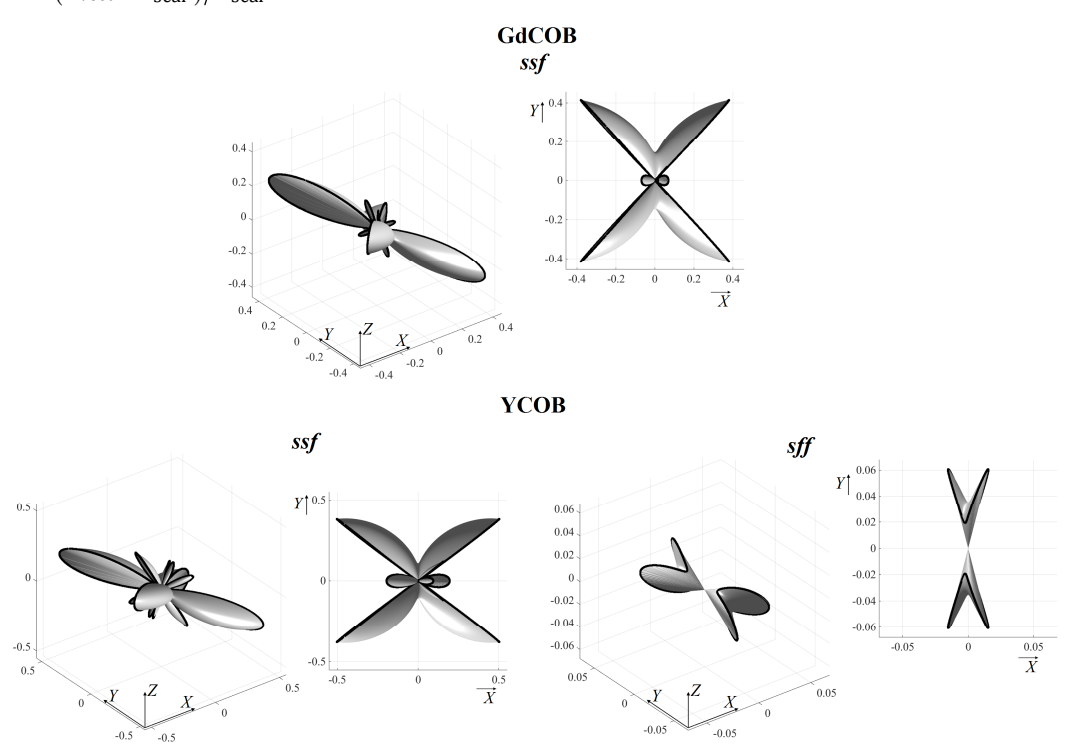


Fig. 4. Extreme surfaces for SHG in monoclinic crystals of point symmetry group m, in pm²/V².

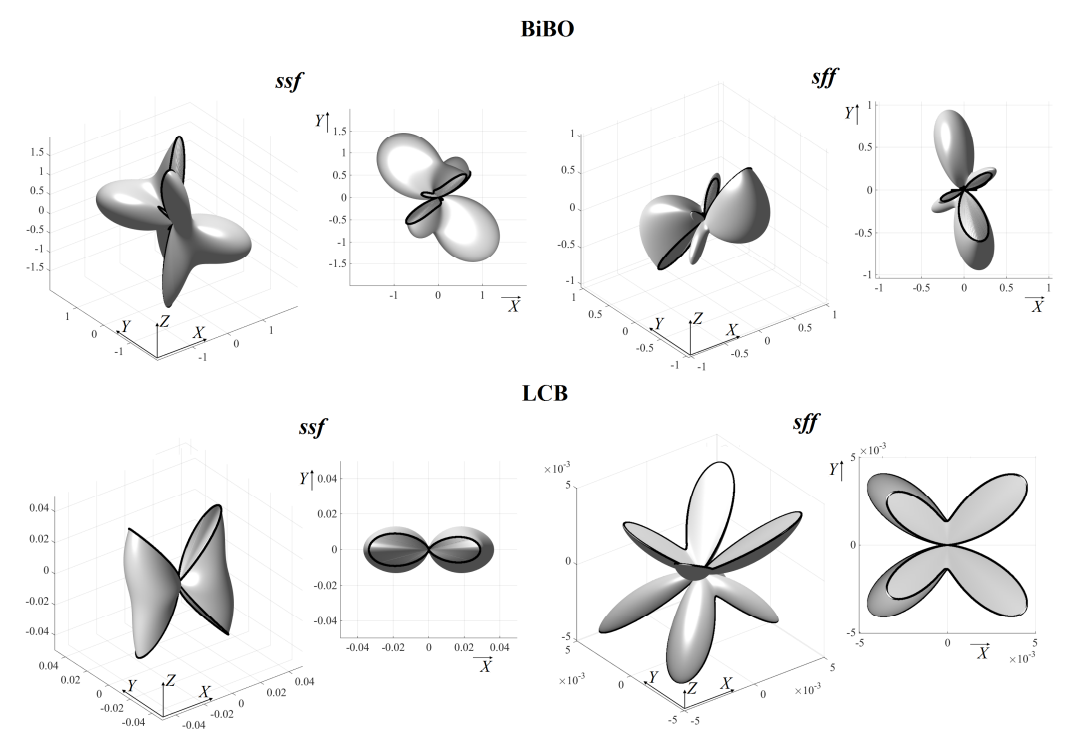


Fig. 5. Extreme surfaces for SHG in monoclinic crystals of point symmetry group 2, in pm²/V².

Table 2. The maximal achievable SHG efficiencies η and corresponding angular parameters.

		Scalar P	M	Vector PM								
Crystal	Angles, deg.		$\eta_{ m scal}^{ m extr}$, $ m pm^2/V^2$	Ang (pump b de	eams),	Ang (SH b de	$\eta_{ m vect}^{ m extr}$, ${ m pm^2/V^2}$					
	$\boldsymbol{\theta}$	φ	F /	$ heta_{1p}, arphi_{1p}$	$\theta_{2p}, \varphi_{2p}$	$\boldsymbol{ heta}$	φ	. ,				
Type I Pl	Type I PM											
GdCOB	113.0	47.6	0.61	coincides with scalar ssf								
YCOB	67.1	142.9	0.68									
BiBO	154.1	42.6	2.0									
LCB	36.6	180	0.056									
Type II Pl	М											
YCOB	98.0	256.0	0.063	82.3	82.2	284	0.064					
ТСОБ	YCOB 98.0 2		0.003	283.5	284.5	82.2	204	(1.4%)				
BiBO	144.9	107.6	1.09	138.1	128.1	133.3	103.2	1.11				
טמוט	144.9 107.0	1.09	99.6	106.5	155.5	103.2	(2%)					
LCB	124.6	220.8	0.0070	almost coincides with scalar sff*								

^{*}the relative increase of SHG efficiency is lower than 1%.

As our calculations show, the use of type I (ssf) vector PM does not allow increasing the efficiency η relative to the scalar PM case for all investigated crystals. In all cases, the lines corresponding to scalar PM in the figure frame the edges of extreme surfaces and pass through the points corresponding to $\eta_{\rm vect}^{\rm extr}$. Practically the same situation takes place in the case of type II (sff) vector PM in YCOB, BiBO, and LCB – the relative increase of SHG efficiency

caused by vector PM is no more than 2%. It is contrary to the case of orthorhombic crystals, where the use of vector PM allows essentially increasing the value of the SHG efficiency, up to several tens of percent for a number of crystals, and even almost one and a half times for $KB_5O_8\cdot 4H_2O$ [2]. The BiBO crystal demonstrates the highest SHG efficiency for both types of PM, whereas LCB shows the lowest.

It should also be noted that accounting for the rotation of the BiBO crystal's optical indicatrix with wavelength changing has practically no effect on the obtained result. For example, the efficiency value obtained without accounting for this rotation differs less than 1% from the value given in Table 2. The maximal relative difference for optimal angles is about 2.3% (the angle θ for ssf PM).

3.2. Sum frequency generation

The results of the efficiency η calculations for some cases of SFG mentioned in [3, 5] are given in Table 3, and the extreme surfaces are shown in Figs. 6–8. As seen in the figures, the shapes of the extreme surfaces differ significantly across wavelength sets for the YCOB crystal. In contrast, for BiBO and LCB, there is a noticeable similarity in the surface shapes at the corresponding PM conditions. For SFG and *sff* PM, using pump waves of different wavelengths allows achieving PM in the GdCOB crystal, where it is absent for SHG.

Table 3. The maximal achievable SFG efficiencies η and corresponding angular parameters.

I avi	Table 3. The maximal achievable SFG efficiencies η and corresponding angular parameters.											
				Scalar PM			Vector PM					
Crystal	λ_1 , μ m λ_2 , μ n	λ2. um	λ_2 , um	λ ₃ , μm	Angles, deg.		η_{scal}^{extr} ,	Angles (pump beams), deg. Angles (SFG beam), deg.			•	η_{vect}^{extr} ,
Cr		77		θ	φ	$\frac{pm^2}{V^2}$	$egin{array}{c} heta_{1p,} \ heta_{1p} \end{array}$	$egin{aligned} heta_{2p,} \ heta_{2p} \end{aligned}$	θ	φ	$\frac{pm^2}{V^2}$	
1	2	3	4	5	6	7	8	9	10	11	12	
					Type l	PM (ssf)						
GdCOB	1.0642	1.9079	0.6831	66.7	145.6	0.79	coincides with scalar ssf					
В	0.5321	1.0642	0.3547	74.9	103.6	0.18	coincides with scalar ssf					
YCOB	1.0642	1.9079	0.6831	67.2	152.5	0.80		coincid	des with s	scalar ssf		
0	0.6594	1.3188	0.4396	150.2	50.5	1.88		coincid	des with s	scalar ssf		
BiBO	1.0642	1.9079	0.6831	158.8	210.8	2.15	í	almost coi	ncides w	ith scalar.	ssf	
m	0.5321	1.0642	0.3547	129.2	0	0.047		coincid	des with s	scalar ssf		
TCB	1.0642	1.9079	0.6831	34.3	180	0.058		coincid	des with s	scalar ssf		
					Type I	I PM (sff)						
GdCOB	1.0642	1.9079	0.6831	96.0	228.6	0.25	95.9 229.4	96.1 227.6	96	228.8	0.25 (2.7%)	
YCOB	1.0642	1.9079	0.6831	93.5	141.4	0.52	93.4 140.5	93.6 142.7	93.5	141.2	0.53 (2.3%)	
5 1.9079 1.0642 0.6831 85.3 84.2 0.041 almost coir					ncides w	ith scalar	sff					

1	2	3	4	5	6	7	8	9	10	11	12
	0.6594	1.3188	0.4396	34.1	288.6	1.09	41.5 273.1	47.5 293.1	43	280	1.15 (6.1%)
0	1.3188	0.6594	0.4396	115.6	100.8	0.96	coincides with scalar sff				
BiBO	1.0642	1.9079	0.6831	159.6	126.9	1.02	142.8 87.6	177.7 117.9	141.5	99.0	1.19 (17%)
	1.9079	1.0642	0.6831	145.9	107.7	1.10	135.4 113.4	131.7 99.3	133.3	104.2	1.14 (11 %)
	0.5321	1.0642	0.3547	112.1	221.5	0.0033	almost coincides with scalar sff				
LCB	1.0642	1.9079	0.6831	137.6	140.0	0.011	136.7 137.6	217.6 221.6	137	219	0.012 (4%)
	1.9079	1.0642	0.6831	112.3	138.9	0.0035	coincides with scalar sff				

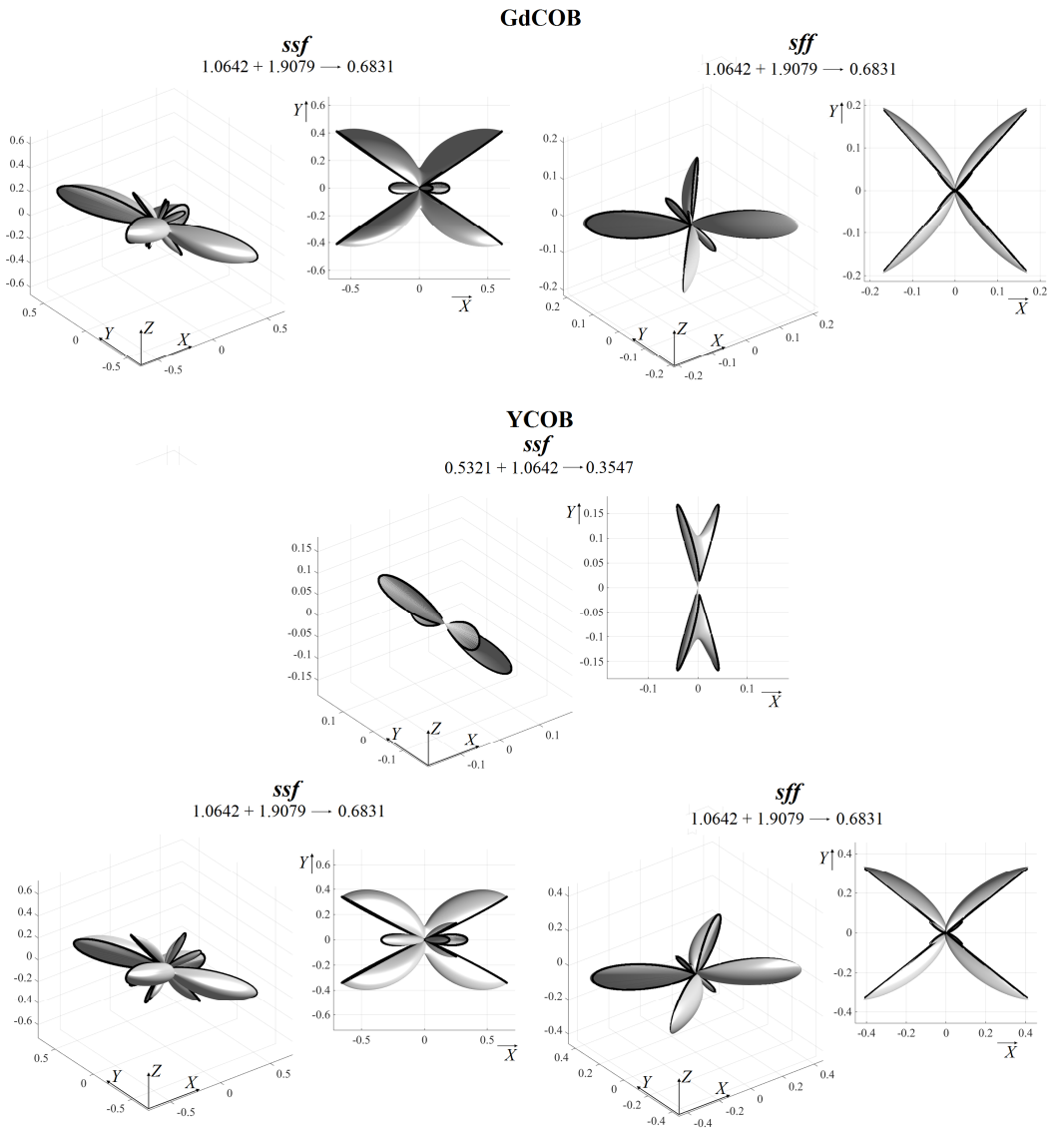


Fig. 6. The extreme surfaces for SFG in monoclinic crystals of point symmetry group m, in pm²/V². The change in wavelengths under interaction is indicated by arrow notation in μ m units.

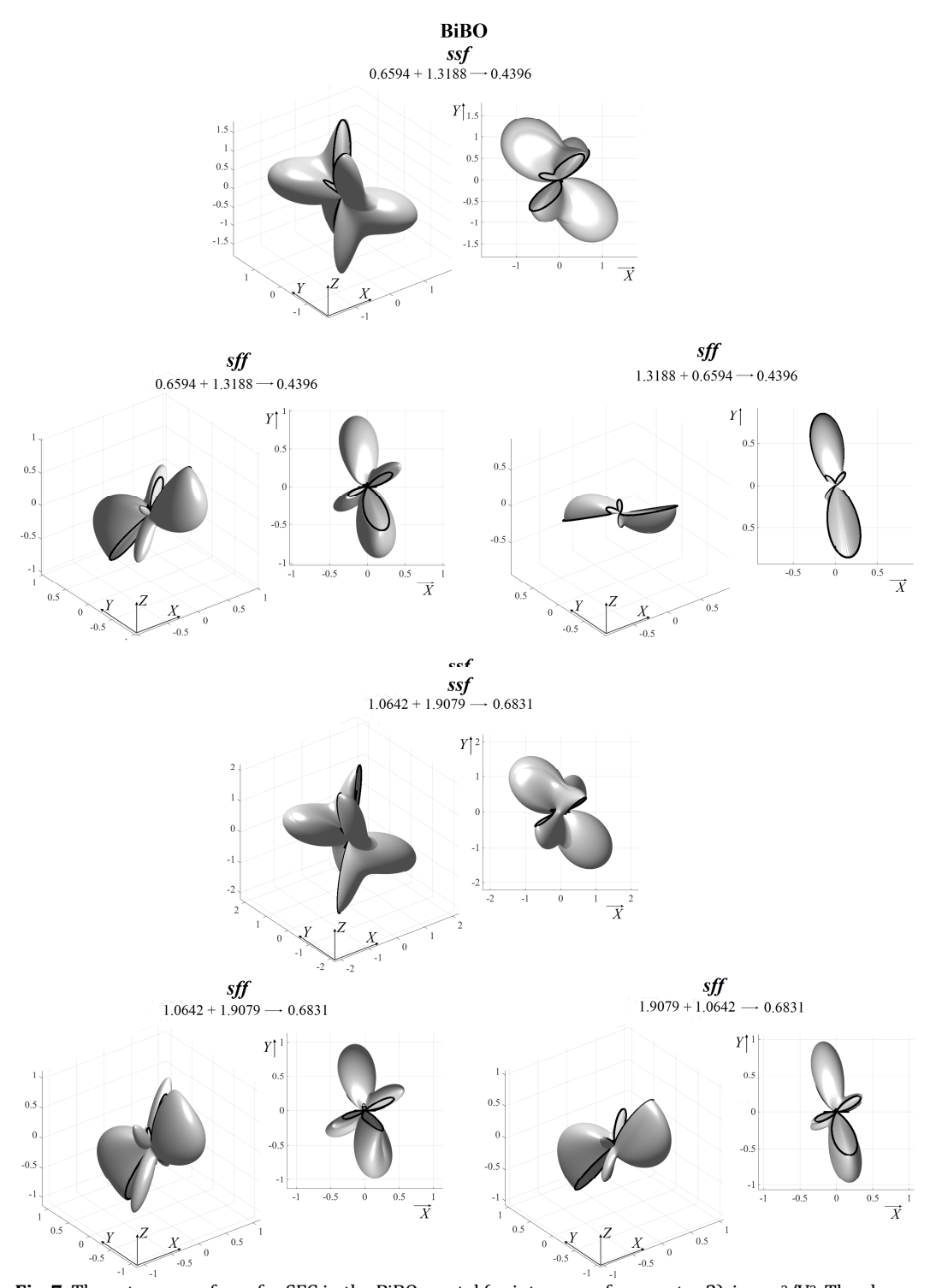


Fig. 7. The extreme surfaces for SFG in the BiBO crystal (point group of symmetry 2), in pm²/V². The change in wavelengths under interaction is indicated by arrow notation in μ m units.

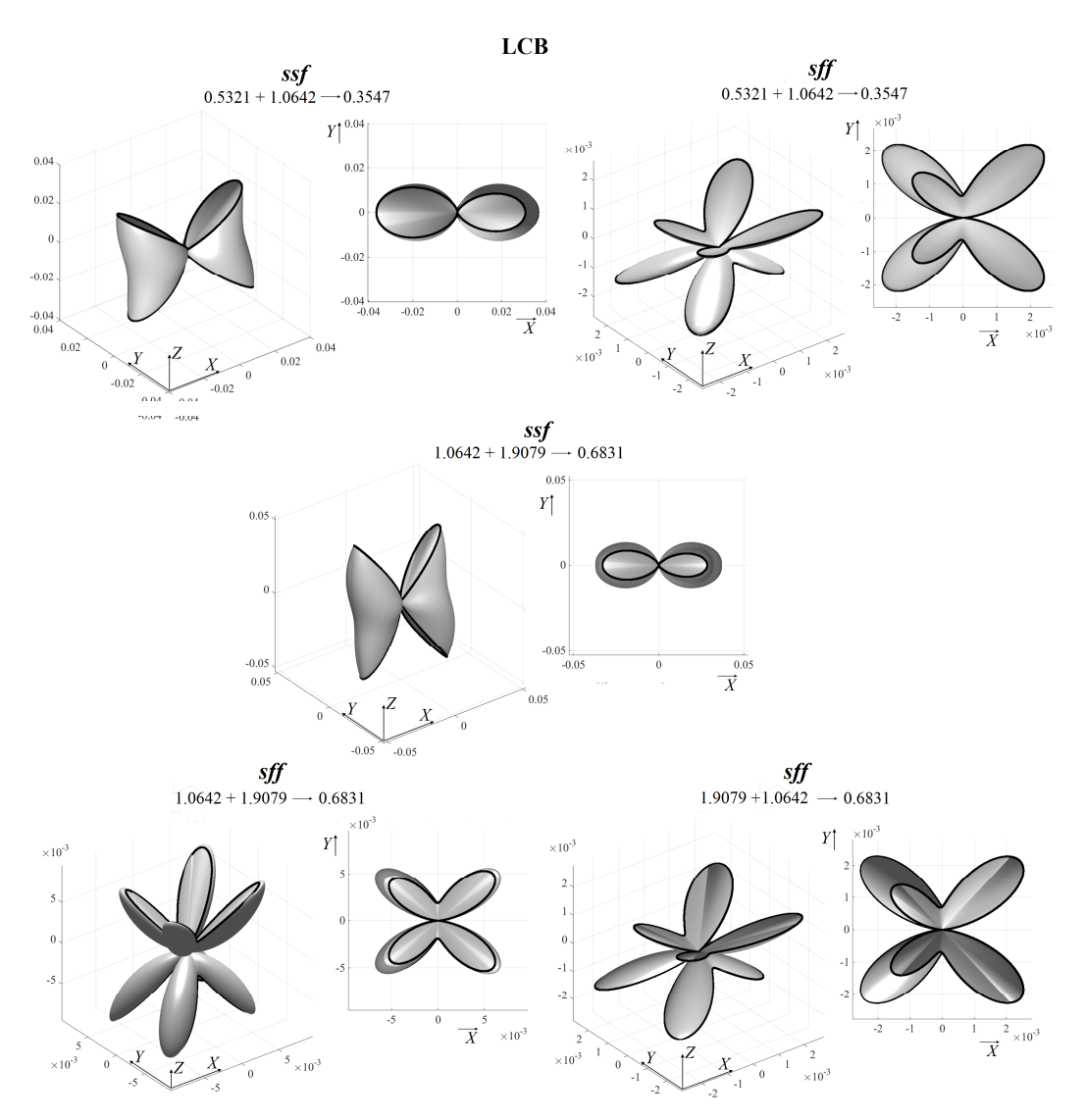


Fig. 8. The extreme surfaces for SFG in the LCB crystal (point group of symmetry 2), in pm 2 /V 2 . The change in wavelengths under interaction is indicated by arrow notation in μ m units.

The results of the optimization are given in Table 3. For brevity, the angle values listed in Table 3 correspond to only one of the equivalent maxima. As shown in Table 3, the highest efficiency is observed for the BiBO crystal across all analyzed PM types. At the same time, the relative increase of SFG efficiency for BiBO is the highest among other crystals (II type PM). However, this excess (about 6%) remains generally insignificant compared with the values observed for orthorhombic crystals [2]. The lowest efficiency values, as well as those for SHG, are demonstrated by the LCB crystal.

Also note that, for the BiBO crystal, in some cases the *sff* PM condition can be satisfied by a mutual change in the input waves' polarization (*fsf* PM or type III PM [5,7,16]). The extreme surfaces for these cases are remarkably different; however, the evolution of the surface in the transition from one type of PM to another can be traced, as was done for the KTA crystal in [2].

3.3. Difference frequency generation

The results of calculations of the efficiency η for difference frequency generation in BiBO and LCB crystals are given in Table 4. For brevity, we do not provide the examples of extreme surfaces (in most cases they are visually similar to the ones shown in Figs. 7,8) as well as the results for GdCOB and YCOB crystals, because the maximum achievable efficiencies η^{extr} (both for scalar and vector PM) for DFG and SFG in these crystals are equal for the same sets of wavelengths. It is the consequence of the Kleiman symmetry rule that is strictly fulfilled for the crystals, i.e. of the fact that the efficiency determined by formula (1) will be the same for the processes $\omega_1 + \omega_2 = \omega_3$, $\omega_3 - \omega_2 = \omega_1$, $\omega_3 - \omega_1 = \omega_2$ in this case (the same situation was occurred for orthorhombic crystals, see [2]).

Table 4. The maximal achievable DFG efficiencies η and corresponding angular parameters.

	λ1,	λ2,	λ3,	Scalar PM			Vector PM				
ital	μm	μm	μm	Angles, deg.	1	$\eta_{ m scal}^{ m extr}$, $ m pm^2/V^2$	Angles (pump beams), deg.		Angles (SFG beam), deg.		$\eta_{ m vect}^{ m extr}$, ${ m pm^2/}$ ${ m V^2}$
Crystal				θ	φ		$egin{array}{c} heta_{1p}, \ heta_{1p} \end{array}$	θ_{2p} , φ_{2p}	θ	φ	V-
1	2	3	4	5	6	7	8	9	10	11	12
Тур	e I PM (<i>ff</i> s	5)									
0	0.4396	0.6594	1.3188	104.2	134.3	3 0.95	74.9 313.8	74.8 314.2	75.0	313.0	0.97 (2.2%)
BiB0	0.4396	1.3188	0.6594	131.2	154.0	2.15	almost c	oincides	with sca	lar <i>ff</i> s	
	0.6831	1.9079	1.0642	141.7	160.8	3 2.47	almost coincides with scalar ffs				
LCB	0.3547	1.0642	0.5321	112.2	81.6	0.010	coincides with scalar ffs				
Э —	0.6831	1.9079	1.0642	42.0	93,3	0.038	coincide	s with sca	alar <i>ffs</i>		
Тур	e II PM (f										
	0.4396	0.6594 (s)	1.3188 (s)	44.6	8.0	0.68	32.8 309.6	31.8 302.3	36.0	323.0	0.89 (30.2%)
	0.4396	1.3188 (s)	0.6594 (f)	62.6	279.9	0.94	almost coincides with scalar fsf				
BiB0	0.4396	0.6594	1.3188	32.6	288.4	1.02	43.4	44.4	43	271	1.23
Bi		(s)	<i>(f)</i>				287.6	295.2			(20.5%)
	0.6831	1.9079 (s)	1.0642 (f)	34.5	287.4	1.09	44.9 283.1	45.6 293.5	45	277.0	1.21 (11.7%)
	0.6831	1.9079	1.0642	35.6	6.8	0.85	150.6	158.3	146	147	1.30
	0.0001	(s)	(s)	00.0	0.0	0.00	142.0	128.0	110		(52.8%)
	0.3547	1.0642	0.5321	129.3	23.4	0.0136	124.2	124.2	124	26	0.0144
		(s)	(s)				22.3	14.8			(5.8%)
В	0.3547	0.5321 (s)	1.0642 (f)	112.1	221.6	0.0033	almost coincides with scalar fsf				
LCB	0.6831	1.9079	1.0642	33.5	218.0	0.015	38.8	39.1	39.0	226.2	0.019
		(s)	(s)				221.2	212.0			(22.1%)
	0.6831	1.9079 (s)	1.0642 (f)	67.7	41.2	0.0034	coincid	es with s	calar <i>fsf</i>		

However, the difference in $\eta^{\rm extr}$ between SFG and DFG in BiBO and LCB can be significant. In particular, the efficiency for DFG ffs PM in BiBO (λ_1 =0.6831 μ m, λ_2 =1.9079 μ m, λ_3 =1.0642 μ m) is equal to 2.47 pm²/V², whereas for the corresponding SFG sff PM it is only 1.19 pm²/V²; for LCB the value of $\eta^{\rm extr}_{\rm vect}$ for DFG fss PM is about 0.014 pm²/V² (λ_1 =0.3547 μ m, λ_2 =1.0642 μ m, λ_3 =0.5321 μ m) and for corresponding SFG ssf PM is 0.047 pm²/V² and so one.

As in the case of SFG, the highest efficiency increase (tens of percent) from vector PM use occurs in the BiBO crystal. Furthermore, among all the crystals studied, BiBO shows the highest efficiency values (obviously due to its high nonlinear susceptibilities; see Table 1), while the lowest values are observed for the LCB crystal.

4. Conclusions

The extreme surfaces technique is used for the determination of the maximal achievable efficiency η of second harmonic, sum and difference frequency generation in monoclinic nonlinear optical crystals GdCOB (GdCa₄O(BO₃)₃), YCOB (YCa₄O(BO₃)₃), BiBO (BiB₃O₆), LCB (La₂CaB₁₀O₁₉) for the case of strict PM. Both vector and scalar PM cases are analyzed and compared for all crystals. The optimal geometries of vector PM, i.e., the directions of the wave vectors of the pump and output beams, that maximize efficiency are determined.

It is shown that, contrary to the previously analyzed case of orthorhombic crystals, the increase in efficiency caused by vector PM is not higher than tens of percent (the maximal value is about 53% for BiBO in the case of difference frequency generation). The highest absolute values of efficiency are also observed for BiBO, ranging from about 0.9 to $2.5 \text{ pm}^2/\text{V}^2$. The lowest efficiency values, for all processes considered, take place for the LCB crystal ($\sim 10^{-3} \dots 10^{-2} \text{ pm}^2/\text{V}^2$).

Acknowledgements and funding. This research received funding from the European Union's Horizon Europe research and innovation program under the Marie Skłodowska-Curie grant agreement No 101086493 — HORIZON-MSCA-2021-SE-01 (project 'TeraHertz'), and was supported by the National Research Foundation of Ukraine (project #2021.01/0410) and the Ministry of Education and Science of Ukraine as part of the project 'Nanoelectronics' (#0123U101695).

Conflict of interest. The authors have no conflicts to disclose.

References

- Andrushchak, N., Buryy, O., Danylov, A., Andrushchak, A., & Sahraoui, B. (2021). The optimal vector phase matching conditions in crystalline materials determined by extreme surfaces method: Example of uniaxial nonlinear crystals. Optical Materials, 120, 111420.
- 2. Buryy, O., Shulha, D., Andrushchak, N., Danylov, A., Sahraoui, B., & Andrushchak, A. (2024). Optimal vector phase-matching conditions in biaxial crystalline materials determined by the extreme surfaces method: the case of orthorhombic crystals. *Applied Optics*, 63(13), 3725-3735.
- 3. Dmitriev, V. G., Gurzadyan, G. G., & Nikogosyan, D. N. (2013). Handbook of nonlinear optical crystals (Vol. 64). Springer.
- 4. Nikogosyan, D. N. (2005). Nonlinear optical crystals: a complete survey. New York, NY: Springer New York.
- Reshak, A. H., Auluck, S., & Kityk, I. V. (2007). Specific features in the band structure and linear and nonlinear optical susceptibilities of La₂CaB₁₀O₁₉ crystals. *Physical Review B – Condensed Matter and Materials Physics*, 75(24), 245120.
- 6. Yariv, A. and Yeh, P. (2002). Optical waves in crystals. New York, Wiley.
- 7. Shen, Y.R. (2002). *Principles of nonlinear optics*. New York, Wiley-Interscience.
- 8. Sirotin, Yu. and Shaskolskaja, M. (1983). Fundamentals of crystal physics. Moscow, Imported Pubn.
- 9. Hellwig, H., Liebertz, J., & Bohatý, L. (1998). Exceptional large nonlinear optical coefficients in the monoclinic bismuth borate BiB₃O₆ (BIBO). *Solid State Communications*, *109*(4), 249-251.
- 10. Hellwig, H., Liebertz, J., & Bohatý, L. (2000). Linear optical properties of the monoclinic bismuth borate BiB₃O₆. *Journal of Applied Physics*, 88(1), 240-244.
- Mougel, F., Aka, G., Salin, F., Pelenc, D., Ferrand, B., Kahn-Harari, A., & Vivien, D. (1999, January). Accurate second harmonic generation phase matching angles prediction and evaluation of non linear coefficients of Ca₄YO (BO₃)₃ (YCOB) crystal. In *Advanced Solid State Lasers* (p. WB11). Optica Publishing Group.
- 12. Aka, G., Kahn-Harari, A., Mougel, F., Vivien, D., Salin, F., Coquelin, P., Colin, P., Pelenc, D. & Damelet, J. P. (1997). Linearand nonlinear-optical properties of a new gadolinium calcium oxoborate crystal, Ca4GdO (BO₃)₃. *Journal of the Optical Society of America B*, 14(9), 2238-2247.

- 13. Andreev, Y. M., Arapov, Y. D., Grechin, S. G., Kasyanov, I. V., & Nikolaev, P. P. (2016). Functional possibilities of nonlinear crystals for laser frequency conversion: biaxial crystals. *Quantum Electronics*, 46(11), 995.
- 14. Wang, G., Lu, J., Cui, D., Xu, Z., Wu, Y., Fu, P., Guan, X. & Chen, C. (2002). Efficient second harmonic generation in a new nonlinear La₂CaB₁₀O₁₉ crystal. *Optics Communications*, 209(4-6), 481-484.
- 15. Wu, Y., Fu, P., Zheng, F., Wan, S., & Guan, X. (2003). Growth of a nonlinear optical crystal $La_2CaB_{10}O_{19}$ (LCB). Optical Materials, 23(1-2), 373-375.
- 16. Fève, J. P., Boulanger, B., & Marnier, G. (1993). Calculation and classification of the direction loci for collinear types I, II and III phase-matching of three-wave nonlinear optical parametric interactions in uniaxial and biaxial acentric crystals. *Optics Communications*, 99(3-4), 284-302.

Shulha, D., Buryy, O., Andrushchak, N., Kohut, Z., Sahraoui, B., Andrushchak, A. (2026). The Optimal Vector Phase Matching Conditions in Biaxial Crystalline Materials Determined by the Extreme Surfaces Method: The Case of Monoclinic Crystals. *Ukrainian Journal of Physical Optics*, *27*(1), 04095–04108. doi: 10.3116/16091833/Ukr.J.Phys.Opt.2026.04095

Анотація. Визначено оптимальні геометрії векторного фазового синхронізму для випадків генерації другої гармоніки, сумарної та різницевої частот у моноклінних нелінійно-оптичних кристалах, а саме: $GdCa_4O(BO_3)_3$, $YCa_4O(BO_3)_3$ (точкова група симетрії т), BiB_3O_6 та $La_2CaB_{10}O_{19}$ (точкова група симетрії 2). Для визначення напрямків хвильових векторів, що забезпечують найвищу ефективність генерації, було використано метод екстремальних поверхонь. Отримані результати порівнюються з результати скалярного фазового синхронізму. Показано, що векторний фазовий синхронізм підвищує ефективність на десятки відсотків порівняно зі скалярним випадком (близько 53% для кристала BiB_3O_6). Кристал BiB_3O_6 проявляє найвищі абсолютні значення ефективності, тоді як найнижчі - кристал $La_2CaB_{10}O_{19}$.

Ключові слова: моноклінні кристали, генерація другої гармоніки, генерація сумарної частоти, генерація різницевої частоти, двовісні кристали, геометрія взаємодії, екстремальні поверхні